Journal of Building Engineering 86 (2024) 108683

Contents lists available at ScienceDirect

Journal of Building Engineering

journal homepage: www.elsevier.com/locate/jobe

Towards net-zero emission: A case study investigating sustainability potential of geopolymer concrete with recycled glass powder and gold mine tailings

Ashish Dey [a], Rubaiya Rumman [b,c], Tadesse G. Wakjira [b], Ashish Jindal [d], Ahmed G. Bediwy [e], M. Shahidul Islam [b], M. Shahria Alam [b,f,*], Samer Al Martini [g], Reem Sabouni [g]

[a] Geotechnical Engineer, Canadian Natural Resources Limited (CNRL), 855 2 St SW, Calgary, Alberta, T2P 4J8, Canada
[b] School of Engineering, University of British Columbia, Kelowna, BC, V1V 1V7, Canada
[c] Department of Civil Engineering, Bangladesh University of Engineering and Technology, Bangladesh
[d] Boston Consulting Group, Mumbai, India
[e] Department of Civil Engineering, Lakehead University, 955 Oliver Road, Thunder Bay, Ontario, P7G 1E5, Canada
[f] Distinguished Visiting Research Fellow, College of Engineering, Abu Dhabi University, Abu Dhabi, United Arab Emirates
[g] Department of Civil Engineering, College of Engineering, Abu Dhabi University, Abu Dhabi, United Arab Emirates

A R T I C L E I N F O

Keywords:
Environmental exposures
Waste materials
Glass powder
Mine tailings
Net-zero emission
Geopolymer concrete

A B S T R A C T

This study explores the feasibility of utilizing waste materials, specifically glass powder (GP) and gold mine tailings (MT), as eco-friendly, net-zero emission alternatives in geopolymer concrete production. The optimal material proportions that yield maximum compressive strength are identified using response surface methodology. The optimized concrete mixtures are comprehensively evaluated for three core attributes; namely, fresh-state properties, such as workability and air content; mechanical characteristics, including compressive, flexural, and splitting tensile strengths; and long-term durability, assessed by freeze-thaw resistance and chloride permeability. In the evaluation of fresh-state properties, it was observed that GP improved workability, whereas MT had a decreasing effect due to its increased fineness and greater surface area. The study also revealed that the combined addition of GP and MT notably increased compressive strength by up to 25%, despite the addition of GP alone slightly reducing the mechanical properties. While these waste materials positively influenced flexural and splitting tensile strengths, the impact was less significant compared to that on compressive strength. Furthermore, in critical durability tests that involve 300 freeze-thaw cycles and rapid chloride permeability assessments, mixtures that contain GP and MT exceeded standard benchmarks. The results indicate that the incorporation of GP and MT together not only enhances mechanical properties but also improves durability. These results demonstrate the potential application of GP and MT as sustainable substitutes in concrete production.

1. Introduction

Widely recognized as the most utilized material in the construction industry, concrete is second only to water in terms of global

* Corresponding author. School of Engineering, University of British Columbia, 1137 Alumni Ave, Kelowna, British Columbia, V1V 1V7, Canada.
E-mail address: shahria.alam@ubc.ca (M.S. Alam).

https://doi.org/10.1016/j.jobe.2024.108683
Received 12 December 2023; Received in revised form 25 January 2024; Accepted 29 January 2024
Available online 19 February 2024

consumption [1]. Its popularity stems from diverse advantages such as versatile shaping, cost efficiency, and resistance to fire [2]. However, the production process for ordinary Portland cement (OPC), a key component of conventional concrete, is highly energy-intensive. This production process is also a significant contributor to global warming. For instance, the production of 1 ton or 1000 kg of Portland cement results in approximately 900 kg of CO_2 emissions [3,4]. Furthermore, the cement industry alone accounts for about 6% of global CO_2 emissions [5–7]. Hence, the drive to replace traditional cement with a more sustainable, durable, and economically viable alternative is a key motivator for researchers, scientists, and engineers. However, the ideal new material should balance the mechanical properties of concrete as well as sustainability, durability, and economic feasibility.

Geopolymer concrete has recently gained considerable attention as a low-emission alternative to OPC-based concrete [8,9]. The binder in geopolymer concrete is formed through a reaction between alumino-silicate materials, such as fly ash (FA), slag, or metakaolin, and alkali activators like sodium hydroxide (NaOH) and sodium silicate (Na_2SiO_3) solutions [8,10–12]. This chemical reaction is known as geopolymerization, a process distinct from the hydration reaction of Portland cement [13]. Specifically, geopolymerization involves the transformation of a large amount of the amorphous phase of alumino-silicates into a compact cementitious structure through hydrothermal polycondensation in alkaline conditions. This chemical reaction results in a three-dimensional polymeric chain consisting of Si–O–Al–O bonds [14,15]. In contrast, Portland cement produces calcium silicate hydrate (CSH) gel through hydraulic activity. Geopolymer concrete has demonstrated promising mechanical and durability properties in both short-term and long-term tests [16–18].

In the context of geopolymer concrete, the role of activators such as highly alkaline solutions that comprise positive ions like sodium is crucial for achieving matrix integrity and compressive strength in the concrete. These solutions neutralize the negative charges of aluminum ions that facilitate the polycondensation process. Commonly used activators in geopolymer concrete include NaOH and Na_2SiO_3, as well as potassium hydroxide (KOH) and potassium silicate (K_2SiO_3) [19,20]. The concentration of NaOH or Na_2SiO_3 directly affects the chemical reactions forming the geopolymer matrix [10]. Studies have shown that Na_2SiO_3, in particular, results in more vigorous reactivity compared to other activators, owing to its dissolved silicon particles that uniquely participate in the geopolymerization process [20,21]. Furthermore, sodium silicate is more environmentally friendly as its production consumes significantly less thermal energy than OPC, reducing thermal energy requirements by as much as 350 °C [22].

In addition to alkali activators, the use of precursor materials such as rice husk ash, FA, slag, and metakaolin, is also crucial in the formulation of geopolymer concrete. Geopolymer concrete, incorporating these precursors not only holds the potential for zero carbon emission concreting that meets structural requirements but also offers room for future enhancements [23]. Moreover, there are some other waste materials available which can be incorporated in geopolymer concrete to reduce its carbon footprint and enhance strength and durability. Example of these waste materials include dehydrated cement paste and red mud [24], ceramic waste [25,26], bottle glass waste nanoparticles [27], and FA [28]. Among these, FA, a by-product of coal-fired electric and steam-generating plants, is most commonly used due to its richness in aluminosilicates [28]. However, it is important to note that the primary source of FA is coal combustion, which is a highly greenhouse gas-intensive process. Coal-fired power generation was responsible for emitting 10 gigatons of CO_2 in 2018, which represents roughly one-third of the total energy-related emissions of 33.1 gigatons [29]. Given its environmental impact, many coal power plants are being decommissioned globally [30–32]. This trend jeopardizes the availability of FA and creates an urgent need to identify alternative materials.

In addition to alkali activators and aluminosilicate-rich precursors, the integration of non-degradable waste materials like glass waste and gold mine tailings (MT) in concrete production could offer environmental benefits. Traditional disposal methods for these materials, such as landfilling, pose environmental risks, including water system contamination [33]. For instance, nearly 200 million tons of glass waste are discarded in landfills worldwide each year. Furthermore, the glass industry consumes a significant amount of non-renewable raw materials. The production of 1 kg of glass sheet necessitates 1.73 kg of raw materials and 0.15 m^3 of water [34]. However, given its silica-rich composition, glass waste holds promise as a raw material in sustainable concrete [35,36] and geopolymer concrete production [37,38]. Previous research demonstrated that the use of crushed recycled glass as a substitute for coarse aggregate yields favourable outcomes, particularly at the 10% replacement level [39]. Moreover, the inclusion of glass powder (GP) as a substitute for sand in geopolymer concrete has been shown to enhance its mechanical properties and sustainability [40,41].

Similarly, the mining sector is another industry with a substantial environmental footprint. Annual waste generation from mining operations is estimated to be between 65 and 80 billion tons, with tailings accounting for 10–15 billion tons and the remainder consisting of waste rock [42]. To manage such waste, the industry typically uses tailings dams, dry disposal, in-pit disposal, and paste technology [43,44]. While tailings dams are the most common, they come with significant drawbacks, such as high costs and adverse environmental and health impacts. Previous studies have investigated the possibility of utilizing these tailings, especially fine material smaller than 200 μm, as a substitute for cement or aggregate in concrete production [45,46].

However, there is a lack of research assessing the mechanical and durability properties of geopolymer concrete incorporating GP and MT. Therefore, this study aims to bridge this gap by examining concrete properties such as slump, air content, compressive strength, flexural strength, splitting tensile, and durability using 3 mixtures that were selected from 49 mixtures, identified through response surface method (RSM)-based optimization. Moreover, the compressive strength of geopolymer concrete was investigated under six different conditions with varying exposures, mixing processes, and curing regimes. The optimum condition was identified as heat curing at 80 °C for 24 h followed by moist curing up to 28 days of age, the time at which they were tested. Results from all other tests were based on specimens cured under this specific condition. This case study not only evaluates the mechanical and durability properties but also identifies optimal conditions through RSM-based optimization. The novelty of this study lies in the exploration of geopolymer concrete incorporating GP and MT to effectively address a crucial research gap.

2. Research significance

Despite the advancements in the research on geopolymer concrete and its potential as a sustainable alternative to conventional concrete, there exist notable knowledge gaps that merit further investigation. For instane, there have been several researches performed on concrete incorporating GP [47–50] or MT [51–53] individually and with other substances. However, their combined effect when incorporated into geopolymer concrete has not yet been explored. In this study, a preliminary investigation has been carried out in order to observe the effect of including both GP and MT on fresh, mechanical, and durability properties of geopolymer concrete. The research presented in this study holds significant importance in the current global context of increasing infrastructure demands and the imperative need for sustainable construction practices. It acknowledges the environmental concerns related to the primary source of FA, which is coal combustion [54]. As coal power plants are being decommissioned globally, the study's exploration of alternative materials for geopolymer concrete becomes crucial. Identifying sustainable substitutes for FA is essential for ensuring the continued viability of geopolymer concrete as a low-emission alternative. Furthermore, the integration of non-degradable waste materials, such as GP and MT, into concrete production contributes to the circular economy by repurposing materials that would otherwise pose environmental risks in landfills [55]. The findings of this study have the potential to influence sustainable construction practices, contribute to the reduction of greenhouse gas emissions, and inspire further research and development in the field of eco-friendly construction materials.

3. Experimental program

3.1. Materials

Class F FA, as shown in Fig. 1a, was used as the main binder component for geopolymer concrete in this study. Its chemical composition and physical properties are presented in Table 1. The oxide composition presented in the table was obtained by a Bruker S2 PUMA ED X-ray Fluorescence (XRF). Locally sourced coarse aggregate with a maximum nominal size of 20 mm was utilized. This aggregate had a specific gravity of 2.71 and a water absorption rate of 2%. To maintain a slump range of 100 ± 20 mm, a polycarboxylate based high-range water-reducing admixture (HRWRA) was added, conforming to ASTM C494/C494M − 17 [56] Type F specifications. An air-entraining admixture was also incorporated to achieve a fresh air content of 6 ± 2%. The fine aggregate used was well-graded river sand with a specific gravity, absorption rate, and fineness modulus of 2.53, 1.5%, and 3.24, respectively. The gradation curves for the aggregates, obtained in compliance with the Canadian Standards Association (CSA) A23.2-2A-19 [57], met the specifications outlined in CSA A23.1 [57], as illustrated in Fig. 2.

Recycled GP samples were produced by crushing discarded glass bottles, including those used for wine and pickles, sourced from the Glenmore landfill site in Kelowna, BC, Canada. The waste glass bottles underwent a grinding process for approximately 24 h in a laboratory ball mill. This grinding procedure was conducted with the aim of achieving a particle size smaller than 75 μm. The details of the process of producing GP from waste glass are described in a previous study performed by the same research group [58]. A laser diffraction technique was employed using Malvern Mastersizer to analyze the particle size distribution of the GP and its gradation is shown in Fig. 3. Table 1 illustrates the oxide composition obtained through XRF analysis.

The MT samples procured from the San Gold Mine, situated 250 km northeast of Winnipeg, Canada. These tailings, which resembled sand in size but were darker and finer, were used as a substitute for sand in the geopolymer concrete formulation. The images of the GP and MT used in this study are illustrated in Fig. 1b and c, respectively. MT characterization is further detailed in the next subsection. Table 1 illustrates the physical properties of MT obtained in the laboratory. Moreover, the table presents a typical chemical composition of a gold MT sample.

Sodium hydroxide and sodium silicate solutions were combined and used as alkaline activators. Different concentrations of NaOH were prepared by blending 99% pure pellets with deionized water before mixing. The chemical composition of the Na_2SiO_3 solution comprised 9% Na_2O, 28% SiO_2, and 63% H_2O with a SiO_2-to-Na_2O ratio of 3.11. It is worth mentioning that the water-to-solid (w/s) ratio was kept at 0.35, and the total binder was 400 kg/m^3. The water content in the mixtures was calculated by considering both the originally added water and the water present in the sodium hydroxide and sodium silicate solutions. Similarly, the total solid content was computed as the combination of the FA, GP, MT, and solid contents in the alkaline activators.

3.2. MT characterization

The moisture content of the MT in its stockpile state was determined as the percentage of the MT's weight in the oven dry state and

Fig. 1. (a) Class F fly ash, (b) glass powder, and (c) mine tailings.

Table 1
Chemical composition and physical properties of FA, MT, and GP.

	Chemical composition (%)							Physical properties		
	SiO_2	Al_2O_3	Fe_2O_3	CaO	MgO	SO_3	Na_2Oeq	Specific gravity	Mean particle size (μm)	Fineness (m^2/kg)
FA	55.20	23.13	3.62	10.81	1.11	0.22	3.21	2.12	16.56	290
MT [87]	77.30	4.48	6.14	9.59	–	1.13	–	2.75	0.29	586.7
GP	71.00	8.00	0.90	8.50	0.38	–	9.80	2.72	15	305

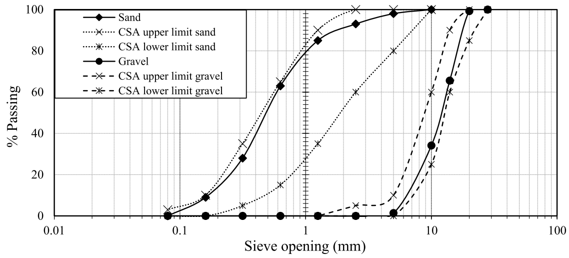

Fig. 2. Particle gradation curve of gravel and sand.

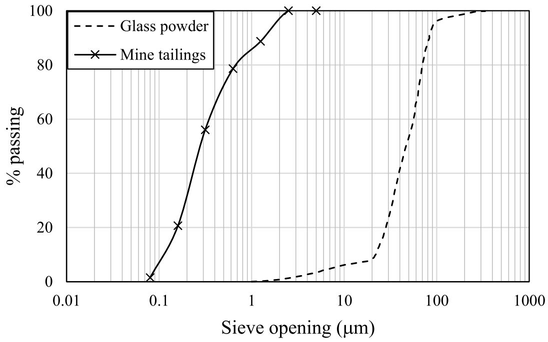

Fig. 3. Particle gradation curve of the waste materials used.

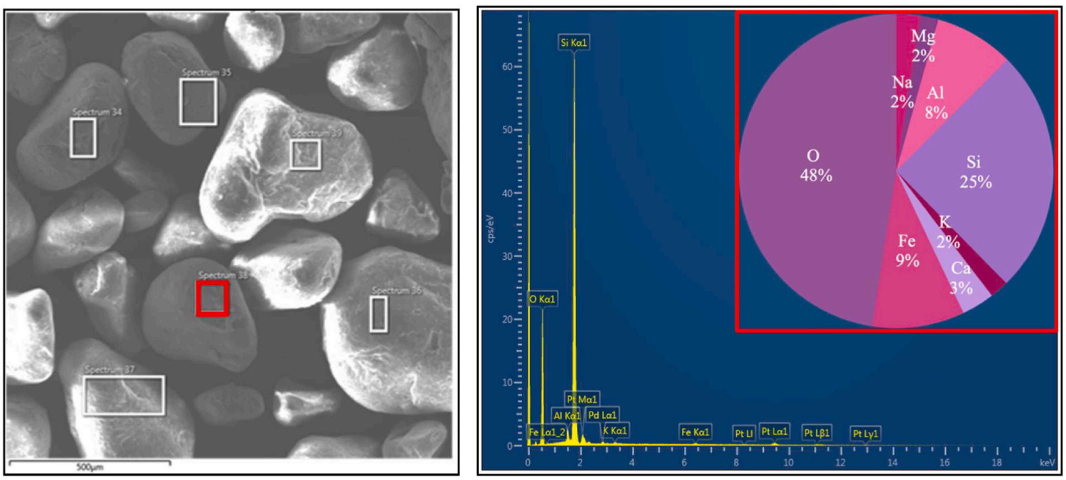

(a) (b)

Fig. 4. (a) SEM of MT sample, (b) EDX spectrum for one point with red square.

was found to be 2.1%, which underscores its high water absorption capacity. The laser diffraction method using Malvern Mastersizer was employed to determine the gradation curve of MT and is shown in Fig. 3. Approximately 95–98% of the MT consists of particles smaller than 3 μm. The particle size distribution is usually described by the median (D_{50}) diameter, which represents the cumulative passing percentage smaller than 50%. The D_{50} was computed to be 0.29 μm (comprising very fine particles). These finer particles increased the specific surface area (5867 cm^2/g), which had an adverse effect on the workability of the mixtures containing MT, as discussed in a subsequent section.

Moreover, the surface morphology of the material was observed using a scanning electron microscope (SEM). A TESCAN Mira 3 XMU SEM at the University of British Columbia was utilized to examine the MT's surface morphology, which would enhance the interpretation of the MT-based geopolymer concrete behavior. A small sample was imaged, mounting on a metal stub using a sticky carbon disk, at 200x magnification, as shown in Fig. 4a. The SEM image revealed that the MT particles possess a smooth surface with approximately irregular rounded or bumpy shapes and different sizes. The elemental composition of the MT was determined using an Oxford Instruments X-Max EDX detector at various locations on the MT particles, as shown in Fig. 4b. The pie chart in Fig. 4b illustrates the computed average elemental composition of the spectrum across all locations. Oxygen was the most abundant element at 48%. Besides, the results showed high content of silicon (Si), aluminum (Al), and iron (Fe), with these elements totalling 42%. In addition, the results confirmed that the content of the toxic metals in the MT sample is quite infinitesimal.

The quantitative phase analysis of the MT was conducted using a continuous-scan x-ray diffractometer (XRD, Bruker AXS Inc, Model D8 equipped with a Fe filter foil, 0.6 mm (0.3°) divergence slit, incident, and diffracted beam Soller slits, and a LynxEye-XE detector). The XRD spectrum was collected over a two θ range of 3–80° with Cu Kα radiation. In addition, the long fine-focus Cu x-ray tube was operated at 35 kV and 40 mA, using a take-off angle of 6°. The XRD data were refined using Bruker's Rietveld program Topas 4.2 software. The obtained XRD pattern is shown in Fig. 5, and the chemical composition is illustrated by the pie chart in the same figure. It is observed that the main material compounds of the MT are quartz (SiO_2), albite ($NaALSi_3O_8$), ankerite, and muscovite at 33, 23, 19, and 12%, respectively. However, other minerals such as calcite, clinochlore, and paragonite exist in the MT sample in small amounts.

3.3. Mixing procedures

Geopolymer concrete requires a special sequence of mixing to ensure a consistent dispersion of ingredients. Firstly, the liquid phase was prepared 24 h prior to the casting. The sodium hydroxide and sodium silicate solutions were blended with water for 5–6 minutes using a hand mixer. A few minutes before the casting, the chemical admixtures (the air-entraining agent and the HRWRA) were mixed with water. The FA, GP, MT, and gravel were then stirred in the dry state in the mixer at a speed of 300 rpm for 3 minutes. The pre-prepared liquids were gradually added to the mixer and mixing continued for 5 minutes until a homogenous mixture was achieved. After mixing, the geopolymer concrete was poured into the molds in three layers and compacted with a steel rod 8–10 times per layer. The molds were initially cured at an elevated temperature of 80 °C and were kept in the oven for 24 h. Then, the specimens were carefully removed and preserved in the curing chambers for the rest of the 28 days when the samples would be tested for compressive strength. This scheme was selected based on trial tests that will be illustrated later in the text, following ASTM C511-21 [59].

3.4. Design of experiment (DOE)

Response surface methodology, a robust multivariate statistical approach, was utilized in this study for data analysis [60]. Utilizing statistical models, RSM optimally fits experimental data, which helps to identify key parameters that impact experimental outcomes. This method also aids in optimizing responses to achieve desirable engineering properties at a minimized cost [61]. In accordance with RSM, the central composite design (CCD) was utilized to efficiently reduce the number of experimental runs. CCD is particularly useful for experiments involving quantitative factors, as is the case in this study. Two-level factorial designs were used, represented by +1 and −1 levels of the variable, which signify the high and low values of the data ranges, respectively. A significant level of 5% was considered in the factorial design to reject the null hypothesis, indicating the probability of "Type I″ error, α = 0.05 corresponding to a 95% confidence level. Commercial software Minitab [62] was employed to perform the CCD.

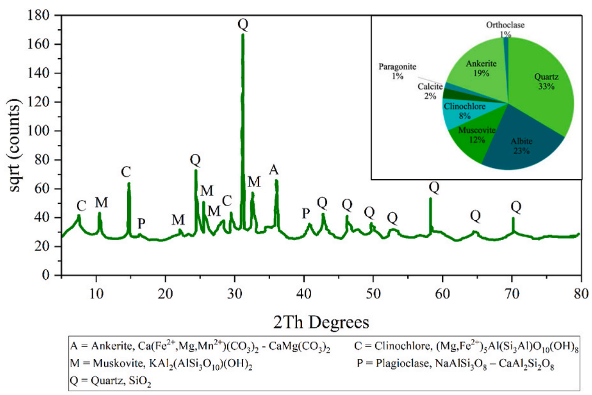

Fig. 5. XRD pattern for MT, Chemical compositions of the MT shown in the pie chart.

The primary parameters included the replacement level of MT, the content of FA in percentage, the concentration of NaOH, and the curing temperature. Table 2 presents the limits and coded values of the variables. These limits have been decided based on the results reported in previous studies. For instance, Borges et al. [63] replaced natural fine aggregate with iron ore MT by 50 and 100%. Sharath et al. [64] also used 100% replacement of fine aggregate with MT. Paiva et al. [65] used 50 and 62% replacement levels of fine aggregate with MT and obtained promising results. Hence, the selection of the replacement percentage for MT in fine aggregate was determined to be between 50% and 75%, guided by insights from previous studies. Various contents of binder in kg/m^3 including 320 [66], 400 [67], 406 [39], and 498 [68] are investigated in the literature. In this study, the FA content was varied between 312 kg/m^3 and 625 kg/m^3 which were represented as percentages of the total binder and aggregate content, the percentages being 15 and 30%. The binder replacement level with GP was selected to be 15% based on the previous research findings [88,89]. Compressive strength was determined experimentally using cylindrical specimens of height 200 mm and diameter 100 mm. These specimens were cast following the standard ASTM C39 [69] and tested at a standard loading rate of 0.33 MPa/s. The total number of mixtures (experimental runs) was determined according to Eq. (1):

$$N = 2^k + 2k + n \tag{1}$$

where N is the total number of experiments, k is the number of parameters considered, and n is the number of replicates (one replicate was considered in this study). There are a total of 31 runs (mixtures) in which 16 experiments represent the factorial design points, 8 experiments represent the axial portion, and 7 experiments represent the center points or confirmatory tests. An experimental test was conducted to determine the compressive strength of the 31 mixes determined by CCD. The results of the response surface experiment design are shown in Fig. 6, which confirmed data normality and test randomness. Fig. 7 shows the normality plot of the standardized effect, where the significant factors are the FA percentage, amount of NaOH, and curing temperature. This observation was confirmed by the Pareto charts obtained from response surface design analysis, as shown in Fig. 8.

3.5. Mixture proportions

Based on the optimization results, three distinct mixtures were cast and subjected to various tests to evaluate their fresh, mechanical, and durability characteristics. The mixture details are presented in Table 3. The mixtures were denoted with the numbers I, II, and III. The amounts of coarse aggregate and activators were kept fixed for all the three mixtures, while the binder and sand amounts varied among the mixtures. For instance, mix I was the control mixture containing 400 kg/m^3 FA and 674 kg/m^3 sand. Mix II contained 340 kg/m^3 FA and 60 kg/m^3 GP replacing the FA. In mix III, along with the same FA replacement with GP, MT also replaced sand by 404 kg/m^3. Hence, the amount of sand used in mix III was 270 kg/m^3.

3.6. Mixing procedures and curing conditions

The three mixture proportions of concrete listed in Table 3 were cast using both hand compaction and an internal vibrator. Moreover, several curing conditions were applied to the three mixtures of concrete in order to observe the effect of curing conditions on their compressive strength. Curing at higher temperatures for activating the geopolymer activators has been observed to result in a better compressive strength in previous studies [70–72]. Besides, temperatures 60 and 80 °C were suggested for the initial heat curing of geopolymers [73]. Therefore, in this study, an elevated temperature of 80 °C was chosen for heat curing the specimens for several durations. All the samples were tested at 28 days after casting. Table 4 presents all the different mixing processes and curing regimes carried out on the mixtures after casting. The conditions are denoted with the alphabets A to F. In one curing condition, the mixtures were cured at an elevated temperature, for instance, 80 °C for 24 h, followed by moist curing for the rest of the 28 days. The same curing conditions were applied for geopolymers with two types of compaction processes; namely, hand mixing (A) or compaction with an internal vibrator (B). Another curing condition was to cure the specimens at 80 °C for 24 h, then dry air curing for the next 7 days and moist curing for the rest of the 28 days. The curing conditions with hand and vibrator compaction are denoted with C and D, respectively. Condition E denotes 80 °C heat curing for 3 days and moist curing for up to 28 days afterwards. The curing condition F was to heat cure at 80 °C for 7 days and moist curing afterwards. Since it was observed from the condition pairs A-B and C-D that the vibrator compaction performed better than hand compaction under the same curing condition, only the compaction with a vibrator was done for conditions E and F.

3.7. Evaluation of fresh, mechanical, and durability properties

The slump test for each mixture was performed immediately after mixing following ASTM C143-20 [75]. A standard truncated cone was filled with fresh concrete in three uniform layers, each compacted with a steel tamping rod. After gently removing the cone, the

Table 2
Limits and coded values of variables.

Parameter	Coded value	
	+1	−1
Mine tailings (%)	75	50
Fly ash (%)	30	15
Temperature (°C)	80	60
NaOH (ml)	380	200

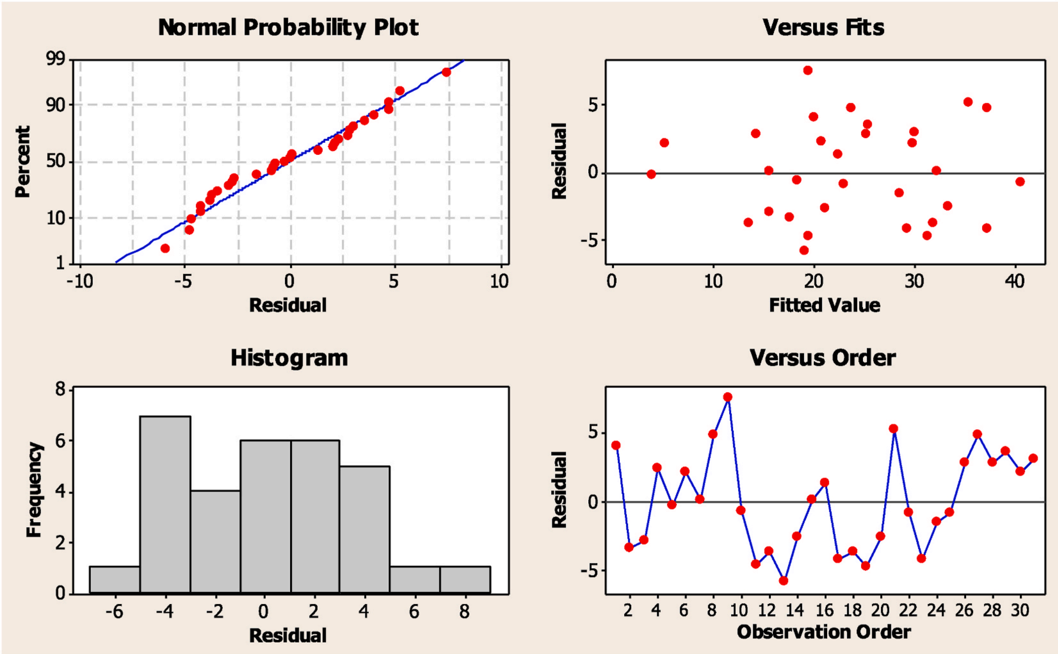

Fig. 6. Response surface (central composite) experiment design output.

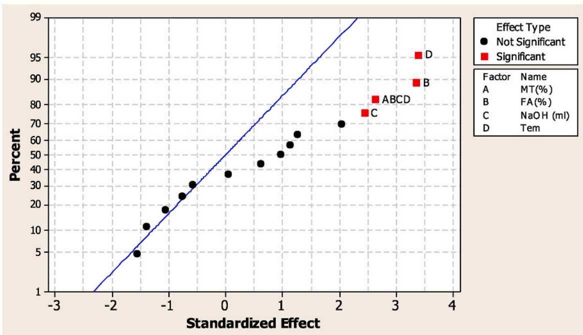

Fig. 7. Normality plot of the standardized effect.

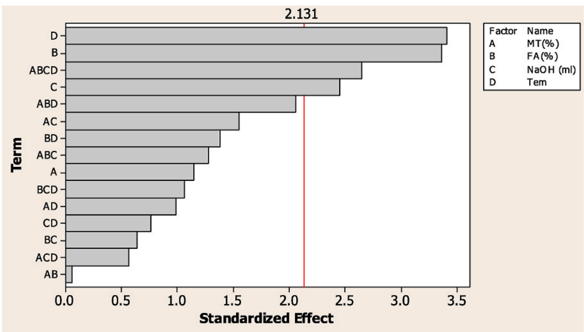

Fig. 8. Pareto chart for the standardized effect of input parameters (Tem: curing temperature).

slump was measured as the difference between the mold height and the average height of the concrete's upper surface.

Air content in the fresh concrete was quantified using the pressure method, as per ASTM C231-22 specifications [76]. Compressive strength was assessed under various curing temperatures using three cylindrical specimens of size 100 × 200 mm, following ASTM

Table 3
Proportions of the mixtures per cubic meter of concrete.

Mixture ID	Binder (kg)		Aggregate (kg)			Activator (kg)		Water (kg)
	FA	GP	Sand	MT	Coarse	Na_2SiO_3	NaOH	
Mix I	400	0	674	0	1010	105	52.5	44.5
Mix II	340	60	674	0	1010	105	52.5	44.5
Mix III	340	60	270	404	1010	105	52.5	44.5

Table 4
Curing regimes of the three mixes of geopolymers.

Designation	Curing condition	Compaction by
A	80 °C heat curing for 24 h, moist curing for up to 28 days	Hand
B	80 °C heat curing for 24 h, moist curing for up to 28 days	Internal vibrator
C	80 °C heat curing for 24 h, dry air curing for 7 days, moist curing up to 28 days	Hand
D	80 °C heat curing for 24 h, dry air curing for 7 days, moist curing up to 28 days	Internal vibrator
E	80 °C heat curing for 3 days, moist curing for up to 28 days	Internal vibrator
F	80 °C heat curing for 7 days, moist curing for up to 28 days	Internal vibrator

C39/C39M-20 [69]. Splitting or indirect tensile strength tests were conducted on 100 × 200 mm cylindrical specimens, following ASTM C496-17 [77]. The maximum tensile stress was calculated using Eq. (2):

$$T = \frac{2P}{\pi l d} \tag{2}$$

where P is the applied load in N, l and d denote the length and diameter in mm, respectively, and T signifies the tensile strength in MPa.

Flexural performance was assessed through four-point bending tests on three standard prisms (100 × 100 × 350 mm), conducted as per ASTM C1609-19 [78]. Flexural strength was determined using Eq. (3):

$$f = \frac{P_f l_f}{b d_f^{\,2}} \tag{3}$$

In this equation, f represents the flexural strength in MPa, P_f is the applied load in N, l_f is the span length in mm, b is the average width at the fracture point in mm, and d_f is the average depth of the specimen at the fracture point, also in mm.

Freeze-thaw (F/T) cycles were applied in line with ASTM C666 procedure A [79], which involves alternating the temperature from +4 °C to −18 °C for freezing and from −18 to +4 °C for thawing. For each cycle, the peak temperature at freezing (−18 °C) and thawing (+4 °C) was maintained for 2 h. The relative dynamic modulus of elasticity was evaluated during the cyclic exposure using the resonance frequency method on the specimens (transverse mode) according to ASTM C215-19 [80].

Finally, the rapid chloride permeability test (RCPT) was conducted in line with ASTM standard C1202-22 [81], as a durability test on concrete to assess the interconnectivity of the pore system. A 50 mm slice was cut from a 100 × 200 mm concrete cylinder and vacuum saturated. It was then placed between two cells: one contained 3% NaCl solution, and the other with 0.3 NaOH solution,

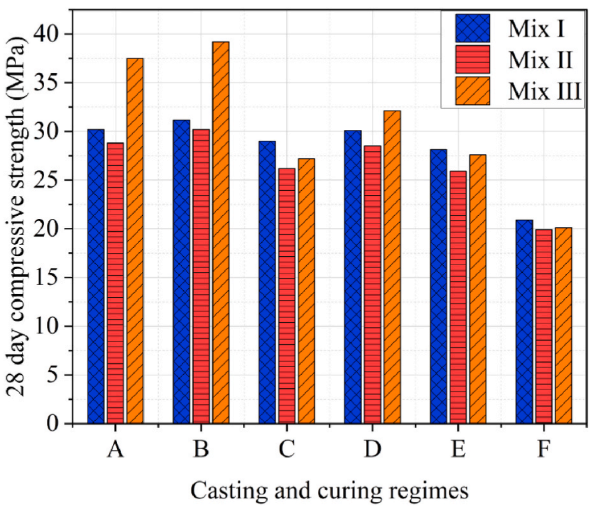

Fig. 9. Compressive strength of geopolymers (Refer to Table 4 for the casting and curing regime designations).

connected to a 60-V voltage source. The total current passed through the saturated pores of the concrete slice was measured after a 6-h duration.

4. Results and discussion

4.1. Optimization of curing conditions based on compressive strength results

Geopolymer concrete often exhibits exceptional engineering properties, and heat curing can contribute to achieving higher compressive strength compared to ambient curing [70–72]. In this regard, geopolymer concrete mixtures with waste materials were subjected to various curing schemes and heating conditions to optimize the ideal mixing and curing conditions, thereby enhancing the compressive strength. The results of compressive strength for the three mixtures under the various curing conditions mentioned in Table 4 are illustrated in Fig. 9. Overall, conditions A and B, where the specimens were heat cured for 24 h and moist cured afterwards, provided the highest strength compared to the rest of the conditions. Comparing all the conditions, mix II provided the lowest strength compared to mix I and mix III. Mix III had the highest compressive strength under conditions A, B, and D. For conditions C, E, and F, mix I provided the highest strength. The highest compressive strength for mixtures I, II, and III were obtained for condition B and the values were 31.16, 30.2, and 39.2 MPa, respectively. In conditions C and D, the samples were heat cured for 24 h similar to that of mixtures A and B. However, they were dry air cured for the next 7 days before putting them in the moist curing chamber. The dry air curing for the 7 days resulted in lowering the compressive strength by 4.0%, 9.0%, and even 27.4% for mixtures I, II, and II, respectively, for hand compacted ones. Moreover, these drops in strength were 3.4, 5.6, and 18.1% for machine compacted mixtures I, II, and II, respectively. The reduction in strength observed due to dry curing can be ascribed to the depletion of essential water needed for hydration reactions, particularly in the initial stages, such as within the first 7 days. Hence, even the moist curing afterwards was not enough to ensure proper strength gain in the geopolymers.

The curing condition pairs A-B and C-D were the same, except for the compaction processes. It is observed from the figure that the mixtures made with internal vibrators provided better strength than their hand compacted pair. For mixtures I, II, and III the increase in compressive strength for compaction with an internal vibrator was 3.1, 4.9, and 4.5%, respectively, compared to manual compaction for conditions A and B. For the C and D conditions, the increase in compressive strength was 3.8, 8.8, and 18.0%, respectively, for mixtures I, II, and III compared to manual compaction. Upon analyzing the results of the compressive strength test, it was established that the optimal exposure condition was attained by compacting with an internal vibrator, followed by 24 h of heat curing. Subsequently, moist curing was applied for the remaining 28 days of the curing period under condition B.

Under condition B, the control geopolymer concrete (mix I), without any waste materials, yielded a compressive strength of 31.16 MPa. The addition of GP to the matrix in mix II decreased the compressive strength slightly by 3.1%. This finding aligns well with results reported by previous studies [37,82,83]. The unreacted GP in mix II diminished the cohesion of the blends and increased the weak interface between the GP and gel phase [37]. This, in turn, resulted in a decline in the compressive strength of the geopolymer concrete. Moreover, adding MT in mix III resulted in the highest compressive strength of 39.2 MPa. The strength value is 25.8% higher than that of the control mix I. These results confirmed the role of tailing in improving the compressive strength when it replaces the fine aggregate, as it acts as an inert filler in the matrix [84], which are particles with a maximum particle size of 250 μm. This result demonstrates the positive impact of tailings as an inert filler with a dual role in reducing porosity and promoting heterogeneous nucleation effects. The packing effect enables tailings to occupy the intergranular voids between cementitious grains in the geopolymer mix, thereby reducing porosity and increasing compressive strength (filler/packing effect). In addition, tailings can act as nucleation sites for hydrates in FA, providing a heterogeneous nucleation effect. As per the detailed discussion, condition B emerged as the optimal choice for compressive strength. Therefore, for subsequent testing, the compaction method involving an internal vibrator and the curing condition of 24 h of heat curing followed by moist curing for the remaining 28 days were deemed most effective.

4.2. Fresh properties

Fig. 10 shows the process of concrete mixing and slump measurement. The slump and air content of the optimized mixtures were measured immediately after mixing and the results are illustrated in Fig. 11a. These results represent the averages obtained from the

Fig. 10. Concrete mixing (a) and slump measurement (b).

three samples. To assess the workability of the mixtures, a constant amount of mixing water and chemical admixtures were used. It can be noticed that the inclusion of GP in mix II (120 mm slump) enhanced the slump by 14% compared to the control mixture (mix I with a slump of 105 mm). This increase in the slump may be attributed to the physical properties of the GP particles, such as their smooth surface and low absorption capacity, which resulted in an increase in the fluidity of the mix. Conversely, the inclusion of MT showed some adverse effect on the slump value, causing a slight decrease from 120 mm in mix II to 102 mm in mix III (with MT), as shown in Fig. 11a. This reduction can be attributed to the high specific surface area and absorption capacity of the MT, which increased the water demand needed to lubricate the particles leading to a reduction in the sample's workability.

The air content is defined as the ratio of the volume of the pores in the concrete to the solid or hardened concrete. A noteworthy observation is that all the mixtures, regardless of the inclusion of GP or MT, showed an air content in the range of 5–8%, which align with the Canadian specification [57]. Therefore, the inclusion of waste materials such as MT and GP, either individually or in combination, in mixtures II and III did not result in excessively high or low air content. This maintained suitable workability in terms of air content. The control mixture (mix I) exhibited an air content of 5.2%, whereas the incorporation of GP yielded an increase in the air content in mix II, reaching 6.4% (a 23% increase). This increase could be attributed to a phenomenon caused by the retention of air bubbles by the surface energy of the glass [85]. Consistently, the inclusion of MT in mix III led to an elevation of air content to 7.1%, which might be attributed to the high absorption capacity of the MT, resulting encapsulation of MT particles by a layer of water, thereby leading to a higher air entrapment. A similar trend was reported in a previous study [86], where iron tailings were incorporated to produce ultra-high-performance concrete.

4.3. Mechanical properties: flexural and split tensile strengths

The flexural and splitting tensile strengths of the geopolymer concrete beams and cylindrical specimens, respectively, are presented in Fig. 11b. While the effect of either GP or MT on the flexural strength and split tensile strength was less than their effect on compressive strength, the trend among these three mechanical strength properties was quite similar. Moreover, these results are in direct agreement with the compressive strength of all mixtures reported in the previous section.

In alignment with previous observations, the flexural strength and split tensile strength decreased with the addition of GP. For instance, the control geopolymer concrete specimen (mix I) and the specimen with GP (mix II) showed comparable flexural and split tensile strengths, with a slight difference of about 12% and 7% for flexural strength and split tensile strength, respectively. This reduction happened because the cohesion of the blends in mix II was compromised due to the presence of unreacted glass powder, leading to an escalation in the weakness of the interface between the glass powder and the gel phase. Additionally, the trend of increasing strength, observed with the addition of MT to the matrix, persisted under the flexural and splitting tensile tests. As an example, substituting the fine aggregate with MT in mix III resulted in an increase in the flexural and split tensile strengths of 10% and 14%, respectively, compared to the control mixture (mix I).

4.4. Durability properties

4.4.1. Resistance of concrete to rapid freezing and thawing

As previously mentioned, three replicates of prismatic (50 × 50 × 285 mm) specimens for each mixture were exposed to 300 cycles of freezing and thawing simulating a North American winter [90]. In the initial phase, a visual assessment was conducted to examine the appearance of specimens after completing the 300 cycles, as shown in Fig. 12. To precisely examine the damage caused by the adopted cyclic environmental exposure, the visual rating specified in ASTM C672 (2012) was utilized in this study. This rating varies from 0 (no deterioration/cracks/spalling) to 5 (extreme deterioration/extensive spalling). Based on the assessment, the control mixture (mix I) without any waste materials experienced severe damage after 300 cycles of freezing and thawing, resulting in a visual rating of 5.0. Adding GP in mix II enhanced the resistance to such exposure, where moderate damage was observed (visual rating of 3.0–4.0). Conversely, the addition of MT in mix III significantly increased the specimen's immunity to environmental exposure, leading to only slight spalling, and thus a visual rating of 1.0. The visual ratings of the samples after exposure along with the change in the relative dynamic modulus of elasticity (R_d) for all mixtures was monitored throughout the 300 F/T cycles and results were compared before and after F/T exposures, as shown in Fig. 13. Therefore, the varying degrees of damage observed in the specimens underscore the protective influence of waste material additions, which affirms the potential of GP and MT to mitigate the detrimental effects of cyclic freezing and thawing. This is further supported by the monitored change in R_d value that provides a quantitative measure of the materials' resilience throughout the environmental exposure cycles.

The addition of MT in mix III resulted in less deterioration, only approximately a 9% reduction in R_d over the 300 freezing and thawing cycles, confirming that the damage occurred on the surface of the specimen with no inner cracking (intact core). In contrast, mix I exhibited a significant drop in R_d of about 32.8% from the initial condition, which is in good agreement with the visual assessment. As for mix II, it displayed a moderate drop in R_d of approximately 18.4%, as shown in Fig. 13. The relatively good freeze-thaw durability exhibited by mix II and mix III can be attributed to the matrix densification and pore refinement induced by the small particle size of waste materials that act as fillers.

4.4.2. Rapid chloride permeability test

The rapid chloride permeability test is an indirect measurement of concrete durability, where the test results are presented in terms of total passing charges through the geopolymer concrete disc to determine the penetrability class. The higher the permeability of the concrete sample, the lower its durability is, and vice versa. Fig. 14 presents the average RCPT results for the geopolymer mixtures obtained from testing two replicates. The columns in the figure represent the total charge passed by each of the mixtures. Moreover, the graph is divided into different permeability zones with the help of the horizontal red lines. It is important to note that the higher the

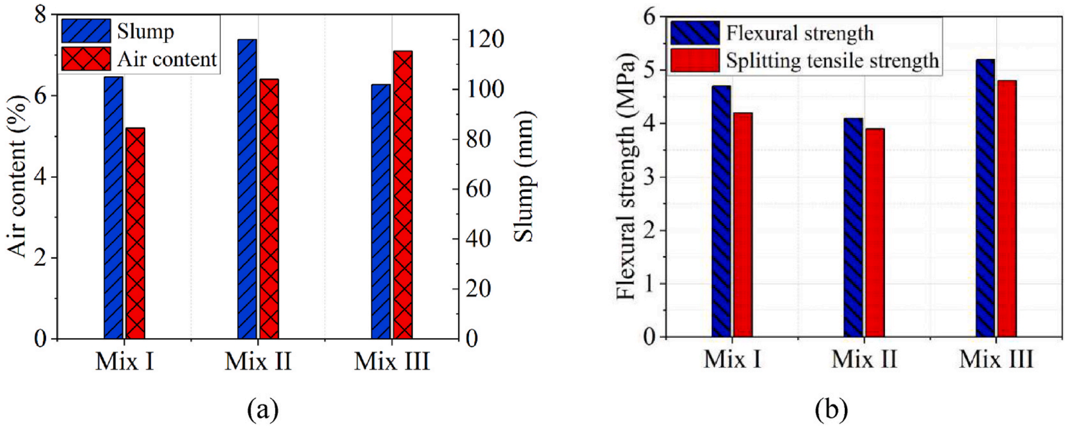

Fig. 11. (a) Fresh properties of geopolymers and (b) Splitting tensile and flexural strength of geopolymers.

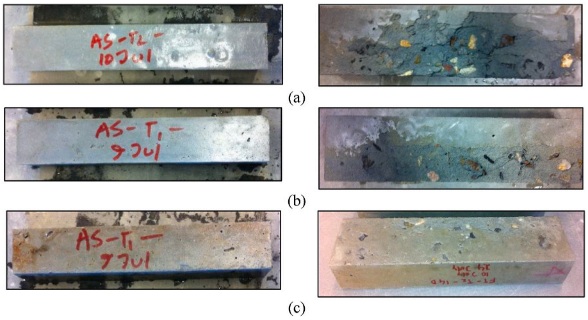

Fig. 12. Visual assessment of different mixtures before and after the exposure: (a) mix I, (b) mix II, and (c) mix III.

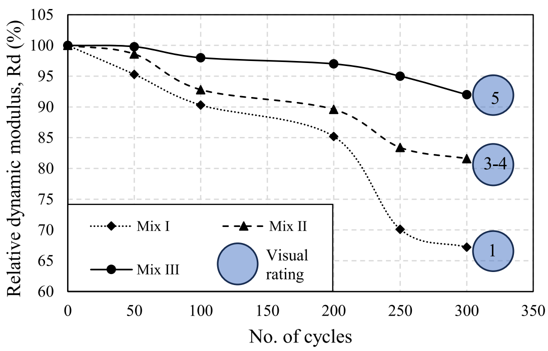

Fig. 13. Change in the relative dynamic modulus of elasticity throughout the cyclic environmental exposure for different mixtures.

passing charges are, the weaker (more permeable and less durable) the concrete is. For instance, following the ASTM C1202 [81], the control mixture without any waste material (mix I) was classified as "high" as the total passed charges was 4120 coulombs, as shown in Fig. 14. Conversely, mix II and mix III showed a permeability class of moderate and low, with total passed charges of 3009 and 1878 coulombs, respectively. These results are consistent with the former R_d findings, which confirmed that the addition of either GP or MT to the geopolymer concrete enhances the durability properties.

5. Conclusions and recommendations

This study assesses the potential of utilizing waste materials, namely GP and gold MT, as alternatives to traditional FA and/or fine aggregates in concrete production, aiming for a sustainable and eco-friendly solution. The investigation focuses on a case study involving three mixtures, one control, one with only GP, and the third incorporating MT with GP, selected using the statistical model

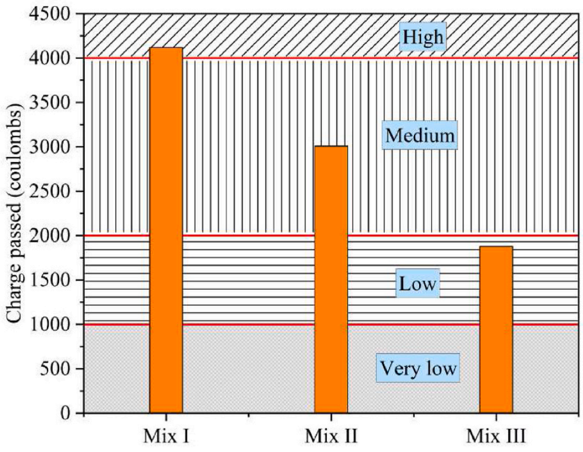

Fig. 14. Rapid chloride permeability test results.

RSM from a pool of 49 options. Six exposure and compaction conditions were applied to all three mixtures, and their 28-day compressive strength results were evaluated. Optimal curing conditions were determined based on compressive strength. The performance of alkali-activated concrete with GP and MT was comprehensively examined for fresh, mechanical, and durability properties, subjected to conditions simulating a North American winter with 300 freeze-thaw cycles. The assessment of optimized mixtures indicates a substantial improvement in overall properties and resistance to harsh environmental conditions. The following conclusions can be drawn from the results of the current study:

- When using a fixed dosage of chemical admixtures, mix II, prepared with the addition of GP, exhibited a greater slump value (enhanced flowability). This result can be attributed to the physical properties of the GP, particularly, a smoother surface and lower absorption capacity. Conversely, the incorporation of MT in mix III reduced the slump by 15% compared to mix II due to MT's high specific surface area. Regardless of whether GP or MT was included, all mixtures showed an air content between 5 and 8%, following the Canadian specification.
- The most optimized curing and mixing conditions for all mixtures, measured by compressive strength, entailed one day of heat curing at 80 °C, followed by moist curing for the rest of the 28 days until the day of the test.
- The addition of GP in mix II slightly reduced the compressive strength of the mixture by 3.1%, which is attributed to the replacement of FA of the geopolymer with unreactive GP. Hence, the strength development was lower. However, the addition of MT as a partial replacement of sand improved the compressive strength by its filler effect due to its small particle size.
- The results of the flexural and splitting tensile strength tests are in direct agreement with the compressive strength of all mixtures.
- Visual analysis showed that specimens containing GP and MT appeared to be more resistant to environmental exposure under cyclic freeze and thaw conditions compared to control specimens.
- Mix II and III performed better in terms of chloride permeability compared to the control concrete, mix I. According to ASTM C1202 [81], mix I was classified in the "high" permeability class. However, mixes II and III demonstrated greater durability, with permeability classifications of "moderate" and "low," respectively.
- The change in the relative dynamic modulus of elasticity for all mixtures was monitored throughout the 300 F/T cycles in which mix I had the highest dynamic modulus reduction (32.8%), mix II moderate (18.4%), and mix III lowest (9%). Waste materials in mixes II and III improved freeze-thaw durability.

In this study, it is crucial to acknowledge certain assumptions and limitations that may impact the interpretation and generalization of the findings. The inherent assumptions associated with the RSM method could have influenced the process of reducing the number of mixture designs from 49 to 3. Additionally, a limitation of this study stems from its nature as a case study, resulting in a simplified experimental program with a minimal number of mixtures due to the deliberately narrow scope. The findings of this study underscore the significant potential of integrating waste materials such as GP and MT into the production of sustainable concrete. This study will serve as a guide for future investigations in this field. However, as a part of future research direction, it is recommended to conduct additional research exploring a wider range of combinations of these two waste materials to determine the optimal dosage. Additionally, there is a critical need for extended research into the life cycle performance of these waste materials within geopolymer concrete to make informed assessments about their overall impact.

CRediT authorship contribution statement

Ashish Dey: Writing – original draft, Visualization, Methodology, Investigation, Formal analysis. **Rubaiya Rumman:** Writing – review & editing, Formal analysis. **Tadesse Wakjira:** Writing – review & editing, Formal analysis. **Ashish Jindal:** Investigation. **Ahmed G. Bediwy:** Writing – review & editing. **M. Shahidul Islam:** Methodology, Investigation. **M. Shahria Alam:** Writing – review & editing, Supervision, Resources, Project administration, Methodology, Funding acquisition, Conceptualization. **Samer Al Martini:**

Writing – review & editing. **Reem Sabouni:** Writing – review & editing.

Declaration of competing interest

The authors declare that they have no known competing financial interests or personal relationships that could have appeared to influence the work reported in this paper.

Data availability

Data will be made available on request.

Acknowledgments

The authors wish to express their gratitude and sincere appreciation for the financial support received from the Natural Sciences and Engineering Research Council of Canada (NSERC). In addition, the assistance received from the technical staff of the Applied Lab for Advanced Materials and Structures (ALAMS) and the School of Engineering at the University of British Columbia (UBC) and PolyRAP Engineered System is gratefully acknowledged. The authors also acknowledge the financial support for this project provided by the Office of Research and Sponsored Programs at Abu Dhabi University under the Distinguished Visiting Research Fellowships program.

References

[1] N. Agarwal, N. Garg, Research on green concrete, IJIRMPS-International J. Innov. Res. Eng. Multidiscip. Phys. Sci. 6 (4) (2018) 362–378.
[2] L. Han, Q. Tan, T. Song, Fire performance of steel reinforced concrete (SRC) structures, Procedia Eng. 62 (2013) 46–55, https://doi.org/10.1016/j.proeng.2013.08.043.
[3] A. Benhelal, G. Zahedi, E. Shamsaei, Bahadori, Global strategies and potentials to curb CO2 emissions in cement industry, J. Clean. Prod. 51 (2013) 142–161, https://doi.org/10.1016/j.jclepro.2012.10.049.
[4] R. Rumman, M. Rubayat, A. Bediwy, M.S. Alam, Partially burnt wood fly ash characterization and its application in low-carbon mortar and concrete, Constr. Build. Mater. 402 (August) (2023) 132946, https://doi.org/10.1016/j.conbuildmat.2023.132946.
[5] K. Gale, N. Mahasenan, S. Smith, Humphreys, The cement industry and global climate change: current and potential future cement industry CO2 emissions, in: Proceedings of the 6th International Conference on Greenhouse Gas Control Technologies, 2003, pp. 995–1000.
[6] K. Nguyen, K. T, N. Ahn, T.A. Le, Lee, Theoretical and experimental study on mechanical properties and flexural strength of fly ash-geopolymer concrete, Constr. Build. Mater. 106 (2016) 65–77.
[7] A.A. Fayomi, G. U, S.E. Mini, O.S.I. Fayomi, Ayoola, Perspectives on environmental CO2 emission and energy factor in cement industry, IOP Conf. Ser. Earth Environ. Sci. 331 (1) (2019).
[8] P.K. Nath, Sarker, Flexural strength and elastic modulus of ambient-cured blended low-calcium fly ash geopolymer concrete, Constr. Build. Mater. 130 (2017) 22–31.
[9] B. Meskhi, et al., Analytical review of geopolymer concrete: Retrospective and current issues, Materials 16 (no. 10) (2023), https://doi.org/10.3390/ma16103792.
[10] M.T. Palomo, M.W. Grutzeck, Alkali-activated fly ashes: a cement for the future, Cem. Concr. Res. 29 (8) (1999) 1323–1329.
[11] J.D. Phair, Van Deventer, Smith, Mechanism of polysialation in the incorporation of zirconia into fly ash based geopolymers, Ind. Eng. Chem. Res. 39 (8) (2000) 2925–2934.
[12] B.V. Hardjito, S.E. Wallah, D.M.J. Sumajouw, On the development of fly ash-based geopolymer concrete, ACI Mater. Journals 101 (6) (2004) 467–472.
[13] D. Ganesan, R. Abraham, R.S. Deepa, Stress–strain behavior of confined geopolymer concrete, Constr. Build. Mater. 73 (2014) 236–331.
[14] W.C.T. Nigel, A.V. Riessen, Determining the reactivity of a fly ash for production of geopolymer, J. Am. Ceram. Soc. 92 (2009) 881–887.
[15] S. Deb, P.K. Sarker, Barbhuiya, Effects of nano-silica on the strength development of geopolymer cured at room temperature, Constr. Build. Mater. 101 (2015) 675–683.
[16] D.M.J. Sumajouw, D. Hardjito, S.E. Wallah, B.V. Rangan, Fly ash-based geopolymer concrete: study of slender reinforced columns, J. Mater. Sci. 42 (9) (2007) 3124–3130.
[17] P. Sarker, Analysis of geopolymer concrete columns, Mater. Struct. 42 (6) (2009) 715–724.
[18] P.K. Sarker, Bond strength of reinforcing steel embedded in geopolymer concrete, Mater. Struct. 44 (5) (2011) 1021–1030.
[19] J. Davidovits, Geopolymer cement a review, in: Geopolymer Institute, Tech. Pap, vol. 21, 2013, pp. 1–11.
[20] M.N.S. Ghafoor, Q.S. Khan, A.U. Qazi, M.N. Sheikh, Hadi, Influence of alkaline activators on the mechanical properties of fly ash based geopolymer concrete cured at ambient temperature, Constr. Build. Mater. 273 (2021) 121752.
[21] M. Komljenović, Baščarević, Mechanical and microstructural properties of alkali-activated fly ash geopolymers, J. Hazard Mater. 181 (2010) 35–42.
[22] L.S. Wong, Durability performance of geopolymer concrete: a review, Polymers 14 (5) (2022) 868.
[23] M. Wasim, A. Abadel, B.H. Abu Bakar, I.M.H. Alshaikh, Future directions for the application of zero carbon concrete in civil engineering – a review, Case Stud. Constr. Mater. 17 (July) (2022) e01318, https://doi.org/10.1016/j.cscm.2022.e01318.
[24] A.A. Abadel, et al., Investigation of alkali-activated slag-based composite incorporating dehydrated cement powder and red mud, Materials 16 (4) (2023), https://doi.org/10.3390/ma16041551.
[25] M. Abd Ellatief, A.A. Abadel, K. Federowicz, M. Abd Elrahman, Mechanical properties, high temperature resistance and microstructure of eco-friendly ultra-high performance geopolymer concrete: role of ceramic waste addition, Constr. Build. Mater. 401 (July) (2023) 132677, https://doi.org/10.1016/j.conbuildmat.2023.132677.
[26] A.A. Abadel, H. Alghamdi, Effect of high volume tile ceramic wastes on resistance of geopolymer mortars to abrasion and freezing-thawing cycles: experimental and deep learning modelling, Ceram. Int. 49 (10) (2023) 15065–15081, https://doi.org/10.1016/j.ceramint.2023.01.089.
[27] Y.R. Alharbi, A.A. Abadel, Engineering properties of high-volume fly ash modified cement incorporated with bottle glass waste nanoparticles, Sustain. Times 14 (19) (2022), https://doi.org/10.3390/su141912459.
[28] L.J. Jaramillo Nieves, F. Elyseu, S. Goulart, M. de Souza Pereira, E.Z. Valvassori, A.M. Bernardin, Use of fly and bottom ashes from a thermoelectrical plant in the synthesis of geopolymers: evaluation of reaction efficiency, Energy Geosci 2 (2) (2021) 167–173, https://doi.org/10.1016/j.engeos.2020.09.004.
[29] IEA, Global Energy & CO2 Status Report 2019, 2019 [Online]. Available: https://www.iea.org/reports/global-energy-co2-status-report-2019/emissions.
[30] A. Cotting, E. Potter, Canada Finalizes Plan to End Most Coal-Fired Power Generation by 2030, S&P Global Market Intelligence, 2018.
[31] B. Storrow, 'Coal's Decline Continues with 13 Plant Closures Announced in 2020', E&E News, Scientific American, 2020.
[32] S. Roth, Coal Plants Are Closing across the West. Here Are the Companies Sticking with Coal, Los Angeles Times, 2020.

[33] Y. Park, A. Abolmaali, Y.H. Kim, M. Ghahremannejad, Compressive strength of fly ash-based geopolymer concrete with crumb rubber partially replacing sand, Constr. Build. Mater. 118 (2016) 43–51.
[34] V. Manikandan, Vasugi, A critical review of waste glass powder as an aluminosilicate source material for sustainable geopolymer concrete production, Silicon 13 (10) (2021) 3649–3663.
[35] A.İ. Çelik, et al., Mechanical behavior of crushed waste glass as replacement of aggregates, Materials 15 (22) (2022), https://doi.org/10.3390/ma15228093.
[36] Ö. Zeybek, et al., Influence of replacing cement with waste glass on mechanical properties of concrete, Materials 15 (21) (2022), https://doi.org/10.3390/ma15217513.
[37] R. Si, S. Guo, Q. Dai, J. Wang, Atomic-structure, microstructure and mechanical properties of glass powder modified metakaolin-based geopolymer, Constr. Build. Mater. 254 (2020) 119303, https://doi.org/10.1016/j.conbuildmat.2020.119303.
[38] A.N. Derinpinar, M.B. Karakoç, A. Özcan, Performance of glass powder substituted slag based geopolymer concretes under high temperature, Constr. Build. Mater. 331 (March) (2022), https://doi.org/10.1016/j.conbuildmat.2022.127318.
[39] Y.O. Özkılıç, et al., The use of crushed recycled glass for alkali activated fly ash based geopolymer concrete and prediction of its capacity, J. Mater. Res. Technol. 24 (2023) 8267–8281, https://doi.org/10.1016/j.jmrt.2023.05.079.
[40] A. Suresh Kumar, M. Muthukannan, K. Arunkumar, A. Chithambar Ganesh, R. Kanniga Devi, Utilisation of waste glass powder to improve the performance of hazardous incinerated biomedical waste ash geopolymer concrete, Innov. Infrastruct. Solut. 7 (1) (2022) 1–12, https://doi.org/10.1007/s41062-021-00694-8.
[41] P. Manikandan, V. Vasugi, A critical review of waste glass powder as an aluminosilicate source material for sustainable geopolymer concrete production, Silicon 13 (10) (2021) 3649–3663, https://doi.org/10.1007/s12633-020-00929-w.
[42] D. Adiguzel, S. Tuylu, H. Eker, Utilization of tailings in concrete products: a review, Constr. Build. Mater. 360 (2022) 129574.
[43] F. Sofrá, D.V. Boger, Environmental rheology for waste minimisation in the minerals industry, Chem. Eng. Journal 8 (2002) 319=330.
[44] O. Bascetin, S. Tuylu, D. Adıguzel, Ozdemir, New technologies on mine process tailing disposal, J. Geol. Sci. 4 (2) (2016) 63–72.
[45] A. Peys, et al., Transformation of mine tailings into cement-bound aggregates for use in concrete by granulation in a high intensity mixer, J. Clean. Prod. 366 (February) (2022) 132989, https://doi.org/10.1016/j.jclepro.2022.132989.
[46] S. Pyo, M. Tafesse, B.J. Kim, H.K. Kim, Effects of quartz-based mine tailings on characteristics and leaching behavior of ultra-high performance concrete, Constr. Build. Mater. 166 (2018) 110–117, https://doi.org/10.1016/j.conbuildmat.2018.01.087.
[47] A.İ. Çelik, et al., Use of waste glass powder toward more sustainable geopolymer concrete, J. Mater. Res. Technol. 24 (2023) 8533–8546, https://doi.org/10.1016/j.jmrt.2023.05.094.
[48] M. P, V. V, Potential utilization of waste glass powder as a precursor material in synthesizing ecofriendly ternary blended geopolymer matrix, J. Clean. Prod. 355 (March) (2022) 131860, https://doi.org/10.1016/j.jclepro.2022.131860.
[49] M. Vafaei, A. Allahverdi, Durability of geopolymer mortar based on waste-glass powder and calcium aluminate cement in acid solutions, J. Mater. Civ. Eng. 29 (10) (2017), https://doi.org/10.1061/(ASCE)MT.1943-5533.0002053 [Online]. Available:.
[50] D.N. Varma, S.P. Singh, 'A Review on Waste Glass-Based Geopolymer Composites as a Sustainable Binder', *Silicon*, 2023, https://doi.org/10.1007/s12633-023-02629-7 [Online]. Available:.
[51] R. Liza, P. Pereyra, J. Rau, M. Guzman, L. Sajo-Bohus, D. Palacios, Assessment of natural Radioactivity and Radon Exhalation in Peruvian gold mine tailings to produce a geopolymer cement, Atmosphere 14 (3) (2023), https://doi.org/10.3390/atmos14030588.
[52] H. Yang, Zhengfu-Zhang, X. Zhou, J. Wang, D. Liu, Simultaneous stabilization/solidification of arsenic in acidic wastewater and tin mine tailings with synthetic multiple solid waste base geopolymer, J. Environ. Manage. 320 (2022), https://doi.org/10.1016/j.jenvman.2022.115783 [Online]. Available:.
[53] X. He, et al., Mine tailings-based geopolymers: a comprehensive review, Ceram. Int. 48 (17) (2022) 24192–24212, https://doi.org/10.1016/j.ceramint.2022.05.345.
[54] J. Ribeiro, T.F. Silva, J.G. Mendonça Filho, D. Flores, Fly ash from coal combustion - an environmental source of organic compounds, Appl. Geochemistry 44 (2014) 103–110, https://doi.org/10.1016/j.apgeochem.2013.06.014.
[55] A.T.M. Marsh, A.P.M. Velenturf, S.A. Bernal, Circular Economy strategies for concrete: implementation and integration, J. Clean. Prod. 362 (October 2021) (2022) 132486, https://doi.org/10.1016/j.jclepro.2022.132486.
[56] ASTM C494/C494M-19, Standard Specification for Chemical Admixtures for Concrete, 2019.
[57] CSA A23.1:19/CSA A23.2:19, Concrete Materials and Methods of Concrete Construction/Test Methods and Standard Practices for Concrete, Jun. 2019.
[58] A. Parghi, M. Shahria Alam, Physical and mechanical properties of cementitious composites containing recycled glass powder (RGP) and styrene butadiene rubber (SBR), Constr. Build. Mater. 104 (2016) 34–43, https://doi.org/10.1016/j.conbuildmat.2015.12.006.
[59] ASTM C511, Standard Specification for Mixing Rooms, Moist Cabinets, Moist Rooms, and Water Storage Tanks Used in the Testing of Hydraulic Cements and Concretes, 2021.
[60] A.A. Abdul Raman, Daud, A Comparison of Central Composite Design and Taguchi Method for Optimizing Fenton Process, Sci. World J., 2014.
[61] A.M. Elemam, A.H. Abdelraheem, M.G. Mahdy, Tahwia, Optimizing fresh properties and compressive strength of self-consolidating concrete, Constr. Build. Mater. 250 (2020) 118781.
[62] A. Alin, Minitab, Wiley Interdiscip. Rev. Comput. Stat. 2 (6) (2010) 723–727.
[63] P.H.R. Borges, F.C.R. Ramos, T.R. Caetano, T.H. Panzerra, H. Santos, Reuse of iron ore tailings in the production of geopolymer mortars, Rev. Esc. Minas 72 (4) (2019) 581–587, https://doi.org/10.1590/0370-44672017720169.
[64] M. Athikkal, B. Das, Some studies on sustainable utilization of iron ore tailing (IOT) as fine aggregates in fly ash based geopolymer mortar, IOP Conf. Ser. Mater. Sci. Eng. 431 (2018) 92010, https://doi.org/10.1088/1757-899X/431/9/092010.
[65] H. Paiva, J. Yliniemi, M. Illikainen, F. Rocha, V.M. Ferreira, Mine tailings geopolymers as a waste Management solution for A more sustainable Habitat, Sustainability 11 (4) (2019), https://doi.org/10.3390/su11040995.
[66] M.W. Ferdous, O. Kayali, A. Khennane, A detailed procedure of mix design for fly ash based geopolymer concrete, in: Proc. 4th Asia-Pacific Conf. FRP Struct. APFIS 2013, No. December, 2013, pp. 11–13.
[67] S. Qaidi, et al., Fly ash-based geopolymer composites: a review of the compressive strength and microstructure analysis, Materials 15 (20) (2022), https://doi.org/10.3390/ma15207098.
[68] M. Olivia, H. Nikraz, Properties of fly ash geopolymer concrete designed by Taguchi method, Mater. Des. 36 (2012) 191–198.
[69] ASTM C39/C39M - 20, Standard Test Method for Compressive Strength of Cylindrical Concrete Specimens, 2020 [Online]. Available: http://www.astm.org/cgi-bin/resolver.cgi?C39C39M-16a.
[70] A.A. Adam, Horianto, The effect of temperature and duration of curing on the strength of fly ash based geopolymer mortar, Procedia Eng. 95 (Scescm) (2014) 410–414, https://doi.org/10.1016/j.proeng.2014.12.199.
[71] Nurruddin, Methods of curing geopolymer concrete: a review, Int. J. Adv. Appl. Sci. 5 (1) (2018) 31–36, https://doi.org/10.21833/ijaas.2018.01.005.
[72] N.K. Verma, M.C. Rao, S. Kumar, Effect of curing regime on compressive strength of geopolymer concrete, IOP Conf. Ser. Earth Environ. Sci. 982 (1) (2022), https://doi.org/10.1088/1755-1315/982/1/012031.
[73] P. Sajan, T. Jiang, C.K. Lau, G. Tan, K. Ng, Combined effect of curing temperature, curing period and alkaline concentration on the mechanical properties of fly ash-based geopolymer, Clean. Mater. 1 (May) (2021) 100002, https://doi.org/10.1016/j.clema.2021.100002.
[75] ASTM C143, Standard Test Method for Slump of Hydraulic-Cement Concrete, 2020.
[76] ASTM C231, Standard Test Method for Air Content of Freshly Mixed Concrete by the Pressure Method, 2022, https://doi.org/10.1520/C0231.
[77] ASTM C496, Standard Test Method for Splitting Tensile Strength of Cylindrical Concrete Specimens, 2017, https://doi.org/10.1520/C0496_C0496M-17.
[78] ASTM C1609/C1609M-19a, Standard Test Method for Flexural Performance of Fiber-Reinforced Concrete (Using Beam with Third-point Loading), 2019.
[79] ASTM C666/C666M-15, Standard Test Method for Resistance of Concrete to Rapid Freezing and Thawing, 2015.
[80] ASTM C215-19, Standard Test Method for Fundamental Transverse, Longitudinal, and Torsional Resonant Frequencies of Concrete Specimens, ASTM Int., 2020, pp. 1–7, https://doi.org/10.1520/C0215-19.2.

[81] ASTM C1202, 'Standard Test Method for Electrical Indication of Concrete's Ability to Resist Chloride Ion Penetration', 2022, https://doi.org/10.1520/C1202-22E01.
[82] N. Sasindran C, V. Jose, Effect of glass powder on geopolymer concrete, Int. J. Sci. Eng. Res. 8 (3) (2017) 1317–1320 [Online]. Available:.
[83] H. Sethi, P.P. Bansal, R. Sharma, Effect of addition of GGBS and glass powder on the properties of geopolymer concrete, Iran. J. Sci. Technol. - Trans. Civ. Eng. 43 (4) (2019) 607–617, https://doi.org/10.1007/s40996-018-0202-4.
[84] R.S. Krishna, F. Shaikh, J. Mishra, G. Lazorenko, A. Kasprzhitskii, Mine tailings-based geopolymers: properties, applications and industrial prospects, Ceram. Int. 47 (13) (2021) 17826–17843, https://doi.org/10.1016/j.ceramint.2021.03.180.
[85] S. García del Toro, D. Alcala-Gonzalez, Más-López, S. García-Salgado, Pindado, Use of ecofriendly glass powder concrete in construction of wind farms, Appl. Sci. 11 (7) (2021) 3050.
[86] X. Zhao, X. Gu, J. Qiu, W. Zhang, Li, Study on the utilization of iron tailings in ultra-high-performance concrete: fresh properties and compressive behaviors, Materials 14 (17) (2021) 4807.
[87] J.P.J. Aseniero, E.M. Opiso, M.H.T. Banda, C.B. Tabelin, Potential utilization of artisanal gold-mine tailings as geopolymeric source material: preliminary investigation, SN Appl. Sci. 1 (1) (2019) 1–9, https://doi.org/10.1007/s42452-018-0045-4.
[88] L. Zhang, Y. Yue, Influence ofwaste glass powder usage on the properties of alkali-activated slag mortars based on response surface methodology, Constr Build Mater 181 (2018) 527–534, https://doi.org/10.1016/j.conbuildmat.2018.06.040.
[89] H. Sethi, P.P. Bansal, R. Sharma, Effect ofAddition ofGGBS and Glass Powder on the Properties ofGeopolymer Concrete, Iran J Sci Technol - Trans Civ Eng 43 (2019) 607–617, https://doi.org/10.1007/s40996-018-0202-4.
[90] P.-C. Aïtcin, 6 - Entrained air in concrete: Rheology and freezing resistance, Editor(s): Pierre-Claude Aïtcin, Robert J Flatt, Science and Technology of Concrete Admixtures, Woodhead Publishing, 2016, 87-95, https://doi.org/10.1016/B978-0-08-100693-1.00006-0.